ISSN 2070-2051, Protection of Metals and Physical Chemistry of Surfaces, 2018, Vol. 54, No. 5, pp. 909–916. © Pleiades Publishing, Ltd., 2018.

PHYSICOCHEMICAL PROBLEMS OF MATERIALS PROTECTION

Spray-Deposition of an Organic/Inorganic Blend for Fabrication of a Superhydrophobic Surface: Effect of Admixing with Silica Aerogel and Modified Silica Nanoparticles[1]

Mehrdad Fallah[a], Mohammad Ghashghaee[b], Ahmad Rabiee[a, *], and Amir Ershad-Langroudi[c]

[a] *Faculty of Polymer Science, Iran Polymer and Petrochemical Institute, Tehran, P.O. Box 14965-115 Iran*
[b] *Faculty of Petrochemicals, Iran Polymer and Petrochemical Institute, Tehran, P.O. Box 14975-112 Iran*
[c] *Faculty of Polymer Processing, Iran Polymer and Petrochemical Institute, Tehran, P.O. Box 14965-115 Iran*
**e-mail: a.rabbii@ippi.ac.ir*

Received April 25, 2017

Abstract—Superhydrophobic and self-cleaning glass slides were fabricated using a facile and low-cost method through spray-coating of four types of blends consisting of stearic acid, the mixture of stearic acid and SiO_2 nanoparticles, the mixture of stearic acid and SiO_2 nanoparticles modified with oleic acid, and the mixture of stearic acid and SiO_2 aerogel onto the surface. The nanocoated surfaces were characterized by attenuated total reflectance Fourier transform infrared spectroscopy (ATR-FTIR), scanning electron microscopy (SEM), energy-dispersive X-ray spectroscopy (EDX), thermogravimetric analysis (TGA), and water contact angle (WCA) measurements. The results have shown that the mixture of stearic acid and SiO_2 nanoparticles modified with oleic acid coating possessed the highest contact angle of about 158.6° and a low sliding angle while the mixture of stearic acid and SiO_2 aerogel had an almost similar WCA but with a more satisfactory durability. In contrast, the stearic acid coating alone had a hydrophobic property and the mixture of stearic acid and unmodified SiO_2 nanoparticles showed superhydrophobic properties without any self-cleaning and durability features.

Keywords: silica aerogel, nanoparticles, spray-coating, superhydrophobic surface, fatty acids
DOI: 10.1134/S2070205118050064

1. INTRODUCTION

Superhydrophobic properties of the solid materials have absorbed many scientists to focus their attention on this field and their applications in industry [1, 2]. The importance of the superhydrophobic surfaces has grown rapidly over the years due to the attractive properties such as self-cleaning, corrosion resistance, anti-icing, anti-biofouling, friction controlling, stain resistance in textiles, reducing the drag resistance, fog condensation, prevention from obstruction of the oil pipes, oil/water separation, etc. [3–12]. Superhydrophobicity is signified by a high water repellency and consequently a high water contact angle ($\theta > 150°$) which is often accompanied with a low water sliding angle ($\theta < 10°$) [13]. A maximum water contact angle (WCA) of about 120° is known to be obtainable over an ideal flat surface [3, 8]. Hydrophobic surfaces fall into two categories according to the value of sliding angle: one called low-adhesive (Cassie state) surface with a low sliding angle and another class named high adhesive (Wenzel state) surface with a high sliding angle to which the water droplets are attached with high adhesive forces. The latter case is also of interest and finds applications, e.g., in liquid transportation [14–16]. Artificial superhydrophobic surfaces are fabricated via two strategies: (1) creation of roughness on an intrinsically hydrophobic substrate, or (2) modification of a rough surface using low-surface-energy materials [7, 17]. Nanoparticles of uniform sizes and favorable chemical features can be synthesized within a Stöber chemistry framework and be applied to control the surface nanoroughness. The deposition of nanoparticles on a microstructured surface using dip coating, spin coating, and spray coating is relatively straightforward and inexpensive [18–20].

The reactive molecules widely employed in the low surface-energy modifications include long-chain fatty acids and thiols, alkyl/fluorinated organic silanes, perfluorinated alkyl agents, polydimethylsiloxane polymers, and their mixtures [3, 10, 21]. The long-chain fatty acids are efficient modifiers thanks to their low surface energy and effective chemisorptions which lead to stable carboxylate groups on the surface [10, 22, 23]. Basic research on superhydrophobic surfaces has mainly focused on rigid solid substrates such as silicon wafers, metal surfaces, and glass slides [24, 25]. It

[1] The article is published in the original.

is meanwhile noteworthy that practical applications of superhydrophobicity depend upon not only the substrate but also the convenience of the treatment techniques [26]. Particularly, the superhydrophobic glass surfaces have created an extensive interest due to their wide applications in the solar panel illumination glasses, car windshields, etc. [14, 27]. To our knowledge, very little information exists in the literature on generating superhydrophobic glass surfaces using nanoparticles and fatty acid modifiers. More specifically, the spray-coating of a glass surface using a mixed layer of a fatty acid with different silica nanoparticles has not been reported. Perhaps, the most relevant work to this research was implemented by Jafari et al. [3] who reported improved contact angles and contact angle hysteresis on an aluminum surface by incorporating nanoparticles of SiO_2 and $CaCO_3$ in stearic acid layers in which silica nanoparticles were superior. In the present work, superhydrophobic surfaces were prepared by spray-coating of silica aerogel and surface-modified silica particles with fatty acid modifiers onto the glass slide substrates for the first time. The wettability, durability, and the physical and textural properties of the surfaces are compared in this paper.

2. EXPERIMENTAL

2.1. Modification of SiO_2 Nanoparticles by Oleic Acid

After drying at 100°C for 12 h in an oven, 1 g of SiO_2 nanoparticles (NanoSav) were dispersed in 50 mL of absolute ethanol under magnetic stirring at 750 rpm for 30 min at room temperature. Then, 0.6 ml oleic acid was added to the solution dropwise at 60°C under constant stirring where the mixture was stirred for 4 h. Afterwards, the sample was filtered and the sediment was rinsed by absolute ethanol and was collected by centrifuge. Finally, the sediment was dried in an oven for 24 h at 100°C.

2.2. Preparation of Superhydrophobic Glass Substrate

A glass slide was employed as the substrate. Prior to the coating, the glass slide was degreased by acetone and washed with deionized water. Then, 1 g of stearic acid was dissolved in 50 mL of absolute ethanol at room temperature and stirred using a magnetic stirrer at 500 rpm for 15 min. A specified dosage of about 0.5 g of silica aerogel (Vakonesh Sanat Part), SiO_2 nanoparticle (Nanosav), or modified nano-silica was dispersed in the stearic acid solution and stirred for 15 min until a homogenous mixture was obtained. Then, the precursor solution was transferred into a spray gun operating at 1.7 bar and room temperature and sprayed onto the clean glass slide surface at an optimized distance of ~15 cm. Finally, the coating was dried at room temperature for 12 h.

2.3. Characterization of the Nanocoated Surface

The surface morphology was explored using a TESCAN VEGA scanning electron microscope (SEM). The elemental composition of the substrate was determined by a TESCAN VEGA3 SBU energy-dispersive X-ray spectroscopy (EDX) apparatus. The attenuated total reflectance Fourier transform infrared (ATR-FTIR) spectra were collected on a Bruker Vertex 80 FTIR spectrometer. The thermogravimetric analysis (TGA) spectra were obtained using Perkin Elmer Pyris 1 apparatus. For obtaining the static water contact angles of the samples, a water droplet of about 12 μL volume was placed on the surface through a needle and the image was taken with a digital camera. Finally, the WCAs were determined from the tangent line and the ellipse curve-fitting to the water droplet image using a Krüss G10 device. For the sliding angle, a water droplet with the same volume was placed on the surface and the slope of the surface was increased until the droplet just began to fall. The angle obtained from the slope of the tilted surface at this moment was registered as the sliding angle.

3. RESULTS AND DISCUSSION

3.1. FT-IR Analysis of Modified Nanoparticles

Figure 1 displays the FT-IR spectrum of the silica nanoparticles modified with oleic acid (OA). This spectrum displayed strong peaks at 2927 and 2855 cm^{-1} which could be assigned [28–31] to the C–H asymmetric and symmetric stretching of aliphatic CH_2 groups, respectively. This figure also shows that long alkyl chain was present in the OA-modified nanoparticles. The peak at 1712 cm^{-1} corresponded to the –COOH group in OA chains and the peak at 1102 cm^{-1} was related to the Si–O–Si bridges. These results established that oleic acid could modify the SiO_2 nanoparticles although the modification was not comprehensive.

3.2. TGA Analysis of Modified Nanoparticles

The percentage of oleic acid grafted on SiO_2 was determined by TGA. Figure 2 depicts the TGA results of the modified nanoparticles. As demonstrated in Fig. 2, a percentage of weight loss of ~3% is observed at temperatures below 150°C which is attributable to the removal of moisture adsorbed on the surface hydroxyl groups of the nano-silica. In a similar work, the researchers [32] studied nano-silica particles obtained from paddy husk ash and their decomposition properties when modified by oleic acid. As they reported, at temperatures below 150°C the nano-silica samples adsorbed ~16% moisture while OA-functionalized nano-silica adsorbed ~7% of moisture. As also mentioned by Premaratne et al. [32], upon functionalization of nano-silica particles with oleic acid, the surface hydroxyl groups form ester bonds with carboxylic

groups of oleic acid making the surface more hydrophobic thus disfavoring the adsorption of water molecules on the surface. The smaller weight loss of our acid-modified samples at temperatures below 150°C with respect to that observed by Premaratne et al. [32] implied a better modification with oleic acid and hence a better hydrophobicity of the modified nanoparticles. The weight loss at the temperatures between 150 to 300°C was ascribed to the dissociation of the non-reacted oleic acid or the detachment of oleic acid chains that have been bonded weakly to the surface of nano-silica [33]. On the other hand, the weight loss at temperatures higher than 400°C is mainly the consequence of the degradation of the chemically bonded organic layer on the surface of the functionalized nano-silica.

3.3. EDX Analysis of SiO_2 Nanoparticles Modified by Oleic Acid

The chemical composition of the silica nanoparticles modified with oleic acid was determined by EDX analysis which operates to the depth of ~3 μm [34]. Elements such as C, N, Na, and Si were present in the SiO_2 nanoparticles as shown in Fig. 3. As can be seen, the amount of carbon atoms was significant. This proved a favorable layering of oleic acid on the SiO_2 nanoparticles.

3.4. Wettability Analysis

The static contact angle and sliding angles of the glass substrates coated in several ways were investigated and the results are shown in Table 1. The contact angle of the sample modified only with stearic acid was 151.0° which increased to 154.0° after the incorporation of the unmodified SiO_2 nanoparticles into the stearic acid layer. The WCA was further elevated to 158.4° and 158.6° with the use of the modified SiO_2 nanoparticles and SiO_2 aerogel in the stearic acid, respectively. These data showed that the incorporation of the modified silica nanoparticles and the silica aerogel could increase the coating contact angle and correspondingly turned the layered surface into superhydrophobic owing to the generation of nanoroughness on the surface. In contrast, the unmodified SiO_2 nanoparticles have several –OH groups that can affect the contact angle negatively, with their most profound influence on the contact angle hysteresis and the durability of the surface (vide infra). The glass plate coated with stearic acid and the mixture of stearic acid and unmodified SiO_2 nanoparticles had a sliding angle above 90° but those coated with stearic acid plus either modified silica nanoparticles or SiO_2 aerogel exhibited very good values ($\theta < 3$) of sliding angle.

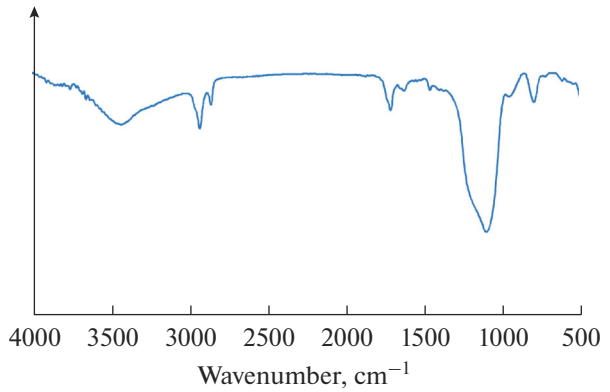

Fig. 1. FTIR spectrum of SiO_2 nanoparticles modified by oleic acid.

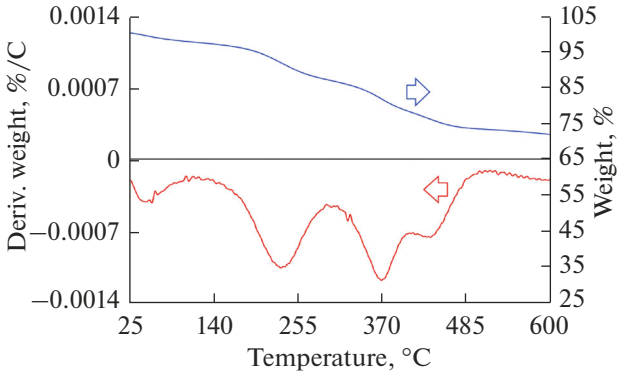

Fig. 2. TGA thermogram of SiO_2 nanoparticles modified by oleic acid.

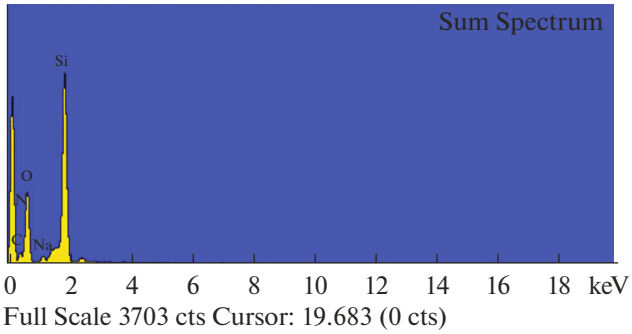

Fig. 3. EDX spectrum of SiO_2 nanoparticles modified by oleic acid.

3.5. ATR-FTIR Analysis

The ATR-FTIR spectra of the glass surfaces coated by different coatings including stearic acid, the mixture of stearic acid and unmodified SiO_2 nanoparticles, the mixture of stearic acid and SiO_2 nanoparticles modified with oleic acid, and finally the mixture of stearic acid and SiO_2 aerogel are shown in Fig. 4. The

Table 1. Water contact angles and sliding angles of the samples with different coatings (degree)

Coating	Stearic acid	Stearic acid + unmodified SiO_2	Stearic acid + modified SiO_2	Stearic acid + SiO_2 aerogel
Static contact angle	151.7	154.0	158.6	158.4
Sliding angle	>90	>90	3	1

absorption infrared spectrum of the stearic-acid-coated sample (Fig. 4a) shows strong peaks at 2929 and 2850 cm^{-1} which were assigned to the C–H asymmetric and symmetric stretching of aliphatic CH_2 groups, respectively [28–31]. The appearance of the mentioned peaks indicated the existence of long-chain alkyl groups on the glass surface. The peaks at 1695 cm^{-1} could be attributed to the vibration of the carboxylic acid C=O bonds [1, 3, 29, 35]. The C–O stretching plus the O–H deformation band appear at 1430 cm^{-1}. Moreover, the Si–O–Si asymmetric stretching and C–O stretching vibration are expected to appear at the frequencies of 1050 and 1065 cm^{-1}, respectively [14, 28, 36–38]. Therefore, the strong peak appeared in the 1000–1100 cm^{-1} region resulted from the overlap of the two peaks. The IR spectra shown in Fig. 4b through 4d for the mixture of stearic acid and different silica particles showed peaks more or less similar to those in Fig. 4a. In fact, all of the coated surfaces had the same functional groups but with varying intensities of their sharp peaks at 1000–1100 cm^{-1}.

3.6. SEM Analysis

The SEM images were used to explore the morphologies of the coated surfaces. As the surface wettability is determined by both the chemical features and roughness of the solid surface, the creation of roughness is a key for the preparation of a superhydrophobic surface. Figure 5 demonstrates the SEM images of the glass slides coated by different coatings. The bare glass had a smooth surface which found enhanced roughness after the deposition of stearic acid and the three nanoparticles. As a result, the energy of the surface decreased with the modifications which is central to create a superhydrophobic surface. Figure 5a shows the glass surface coated with stearic acid. As observed, the glass surface coated almost uniformly but the roughness created by the stearic acid layer was inadequate to have a surface with considerably high contact angle. After the addition of nanoparticles into the stearic acid and spray-coating onto the surface, the desired roughness was achieved. Figure 5b shows the existence of a regular and dense nanostructured unevenness on the surface coated with stearic acid and SiO_2 aerogel. Numerous voids and cracks are evident on the surface which improve the surface roughness. The same property is also seen on Figs. 5c, 5d which relate to the unmodified and modified SiO_2 nanoparticles, respectively.

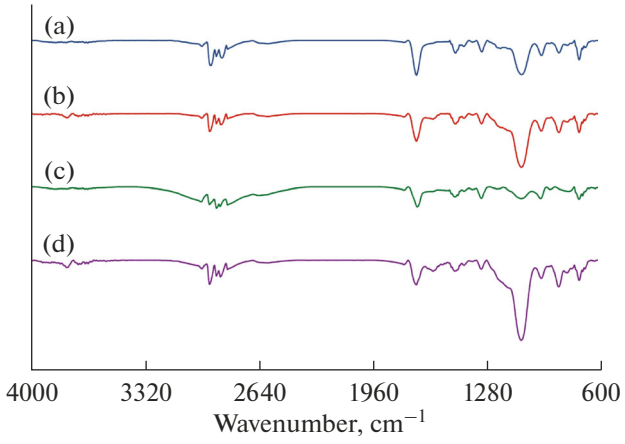

Fig. 4. ATR-FTIR spectra of the coating layers on the glass substrates coated either by (a) stearic acid, (b) stearic acid and SiO_2 aerogel, (c) stearic acid and unmodified SiO_2 nanoparticles, and (d) stearic acid and SiO_2 nanoparticles modified with oleic acid.

3.7. EDX Analysis

The chemical compositions of the glass surfaces modified by different coatings were found using EDX analysis. The EDX mappings were implemented to visualize the elemental constituents and spatial patterns of the carbon and silicon atoms on the glass surface. Figure 6 demonstrates the EDX spectra with the map images of C and Si for the modified glass surfaces. The EDX data presented in Fig. 6a for the sample treated with stearic acid showed that the carbon element was more abundant than the silicon atom on the surface where Si came only from the glass substrate. Figure 6b showed an increased amount of Si with respect to Fig. 6a due to the presence of SiO_2 aerogel, but interestingly with a similar dispersion. This indicates that the superior hydrophobicity of the sample coated with stearic acid plus silica aerogel is not merely the result of a different distribution of the atoms, but the result of a high quality of roughness generated by the aerogel particles and/or the favorably low surface energy created by the partial exposure of the hydrophobic aerogel particles. The highest proportion of silica was observed on the image of the glass

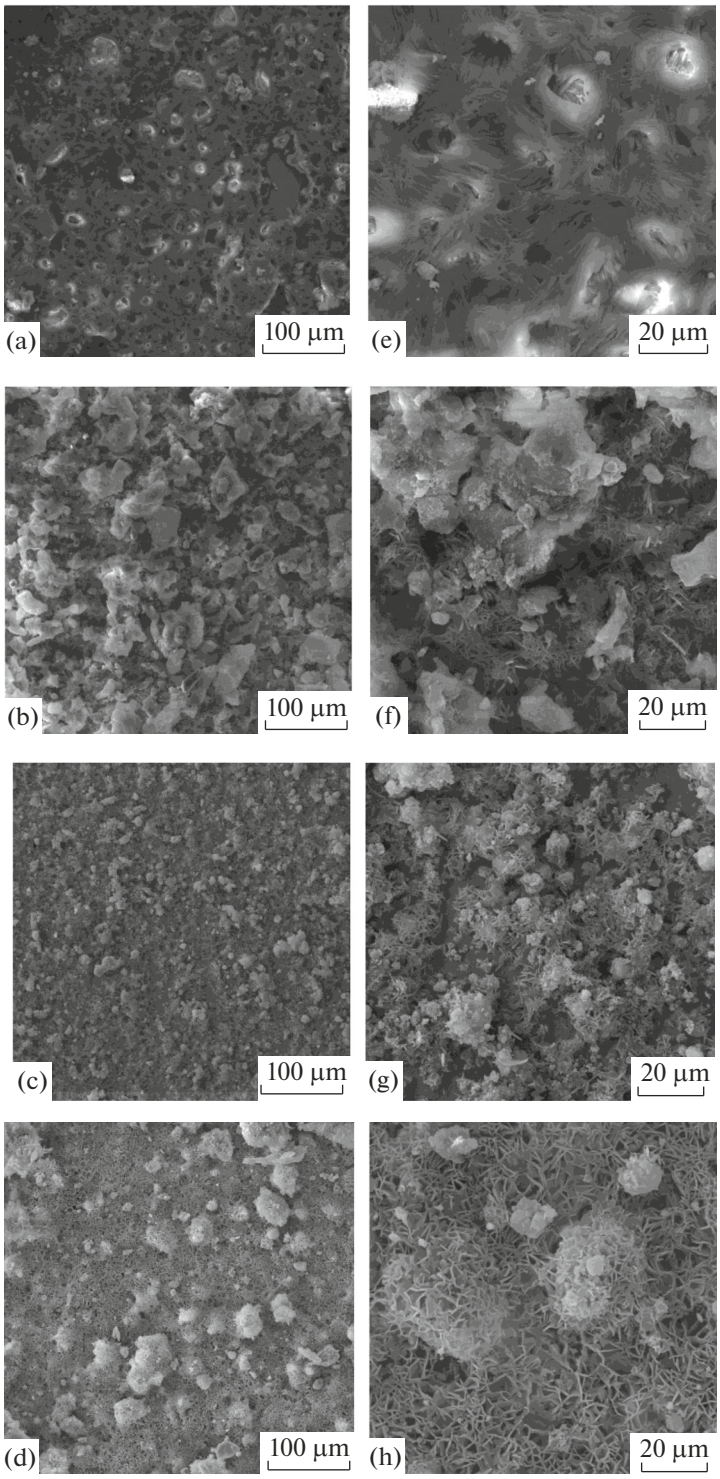

Fig. 5. SEM images of the glass surfaces at two different magnifications of 100 μm (a–d) and 20 μm (e–h) where panels (a) and (e) relate to the glass surface coated by stearic acid, (b) and (f) the samples coated by stearic acid and SiO_2 aerogel, (c) and (g) the glass surface coated by stearic acid and unmodified SiO_2 nanoparticles, and (d) and (h) the glass surface coated by stearic acid and SiO_2 nanoparticles modified with oleic acid.

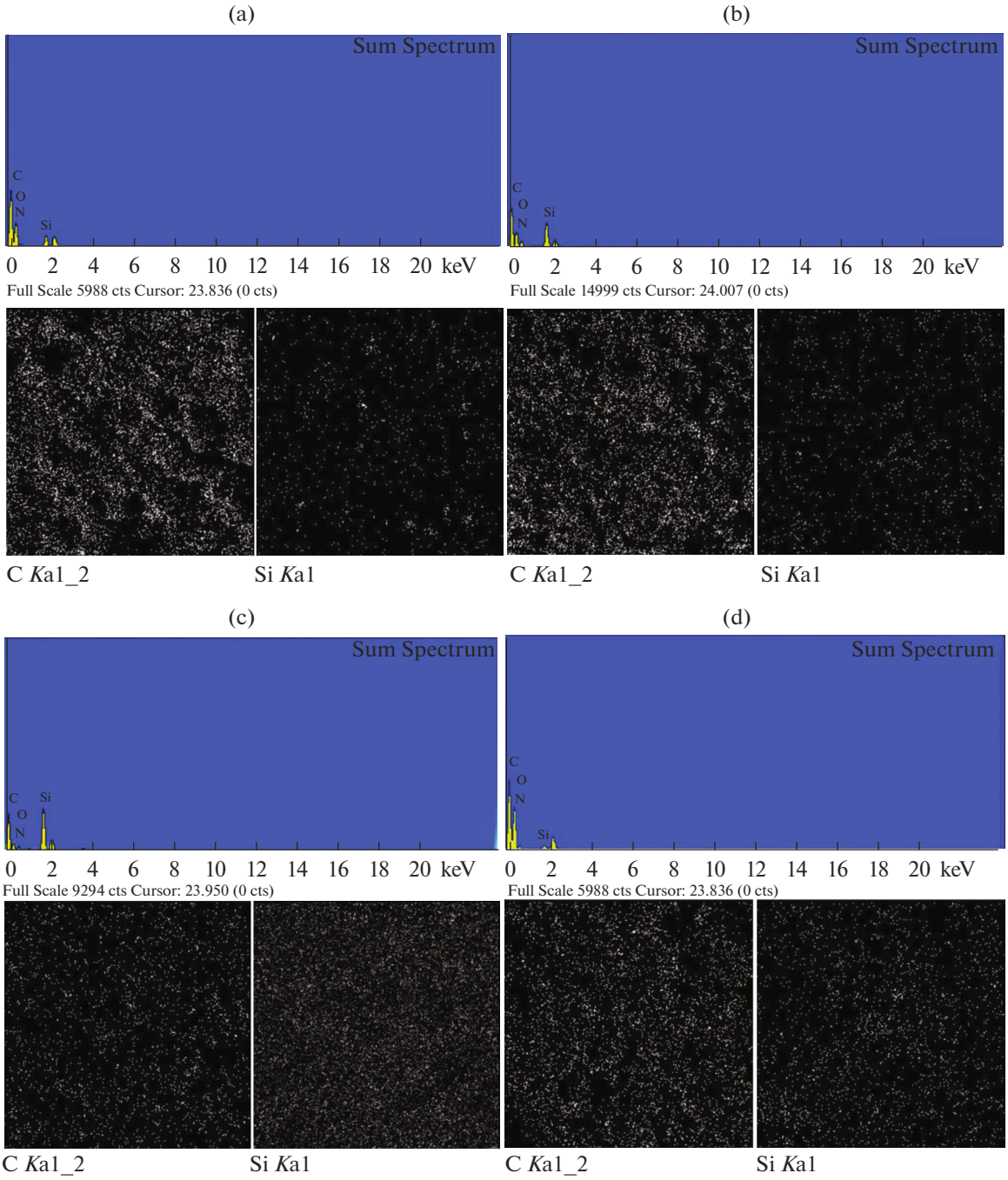

Fig. 6. The EDX spectra with the Si and C mapping images of the glass surfaces modified by (a) stearic acid, (b) stearic acid and SiO_2 aerogel, (c) stearic acid and unmodified SiO_2 nanoparticles, and (d) stearic acid and SiO_2 nanoparticles modified with oleic acid.

surface coated by stearic acid and unmodified SiO_2 nanoparticles (Fig. 6c) where also the Si map indicated a well-dispersed pattern on the surface. A redistribution of elements in favor of C was observed on Fig. 6d due to modifying the silica nanoparticles by oleic acid while still having an appropriate dispersion of Si on the surface.

3.8. Durability of the Superhydrophobic Properties

We have also performed measurements to probe the time-dependent behavior of water droplets on the prepared superhydrophobic glass slides. The dependence of WCA on the contact time is shown in Fig. 7 for the stearic acid-coated sample and the three superhydrophobic samples spray-coated with stearic acid

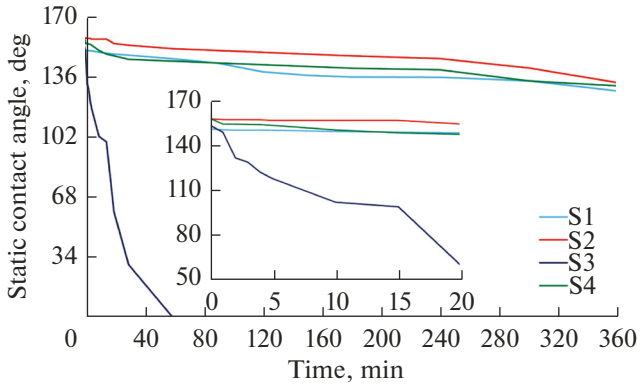

Fig. 7. Alteration of water contact angles with time for different coated surfaces including the glass surface coated by pure stearic acid (S1), the glass surface coated by stearic acid and SiO_2 aerogel (S2), the glass surface coated by stearic acid and unmodified SiO_2 nanoparticles (S3), and the glass surface coated by stearic acid and SiO_2 nanoparticles modified with oleic acid (S4).

and silica. As shown, the WCA decreased steadily for the four samples. The decrease in WCA on the sample coated with pure stearic acid turned the superhydrophobicity of the sample into hydrophobicity within 20 min. Interestingly, the decrease happened more steeply on the sample coated by stearic acid and unmodified SiO_2 nanoparticles. Indeed, the superhydrophobicity of the sample coated with the unmodified SiO_2 nanoparticles turned rapidly into hydrophilicity due to the presence of O–H groups (as a hydrophilic agent) on the surface of nanoparticles. In contrast, the decrease in WCA happened more slowly with the coatings including stearic acid and SiO_2 aerogel or stearic acid and SiO_2 nanoparticles modified with oleic acid due to the assisting hydrophobicity of these nanoparticles. Despite the similar initial situation of the best two samples (S2 and S4 in Fig. 7), the sample which incorporated SiO_2 aerogel was more durable than that including modified silica nanoparticles which experienced an abrupt fall in the initial 10 min. This indicated that although the SiO_2 nanoparticles modified with oleic acid had interacted with the O–H groups under the effect of oleic acid, this interaction/coverage has not been ideal and some of the bindings were soon reversed chemically. For longer times, however, the contact angle deterioration is thought to be primarily affected by the structure, porosity and adhesion of aggregates [39] which is almost similar for both of the samples. This phenomenon was more severely observed in the case of the sample involving the unmodified SiO_2 nanoparticles (S3, Fig. 7).

4. CONCLUSION

Efficient superhydrophobic glass slides were prepared by spray-coating of stearic acid, a mixture of stearic acid and unmodified silica nanoparticles, a mixture of stearic acid and SiO_2 nanoparticles modified with oleic acid, and a mixture of stearic acid and SiO_2 aerogel onto the surface. The results indicated that the mixture of stearic acid and modified SiO_2 nanoparticles had a WCA of 158.6° while the mixture of stearic acid and SiO_2 aerogel showed a WCA of 158.4° both with a self-cleaning property and a promising durability. However, the glass surface with a mixture of stearic acid and SiO_2 aerogel nanocoating had a better durability such that it remained superhydrophobic for a longer time of water contact. Overall, the nanoparticles played an important role in the creation of a promising roughness and consequently the superhydrophobicity and self-cleaning features of the surface.

Funding: This research did not receive any specific grant from funding agencies in the public, commercial, or not-for-profit sectors.

REFERENCES

1. Gao, J., Li, Y., Li, Y., et al., *Cent. Eur. J. Chem.,* 2012, vol. 10, p. 1766.
2. Xi, J., Feng, L., and Jiang, L., *Appl. Phys. Lett.,* 2008, vol. 92, p. 053102.
3. Jafari, R. and Farzaneh, M., *Mater. Sci. Forum,* 2012, vols. 706–709, p. 2874.
4. Zang, D., Zhu, R., Zhang, W., et al., *Corros. Sci.,* 2014, vol. 83, p. 86.
5. Yin, Y., Liu, T., Chen, S., et al., *Appl. Surf. Sci.,* 2008, vol. 255, p. 2978.
6. Huang, Y., Sarkar, D.K., and Chen, X.G., *Nano-Micro Lett.,* 2011, vol. 3, p. 160.
7. Wankhede, R.G., Shantaram, K.T., Khanna, A., and Birbillis, N., *J. Mater. Sci. Eng. A,* 2013, vol. 3, p. 224.
8. Mohamed, A.M.A., Abdullah, A.M., and Younan, N.A., *Arabian J. Chem.,* 2015, vol. 8, p. 749.
9. Liu, C., Su, F., and Liang, J., *RSC Adv.,* 2014, vol. 4, p. 55556.
10. Vengatesh, P. and Kulandainathan, M.A., *ACS Appl. Mater. Interfaces,* 2015, vol. 7, p. 1516.
11. Wang, F., Shen, T., Li, C., et al., *Appl. Surf. Sci.,* 2014, vol. 317, p. 1107.
12. Lu, S., Chen, Y., Xu, W., and Liu, W., *Appl. Surf. Sci.,* 2010, vol. 256, p. 6072.
13. Xie, D. and Li, W., *Appl. Surf. Sci.,* 2011, vol. 258, p. 1004.
14. Rezayi, T. and Entezari, M.H., *Surf. Coat. Technol.,* 2015, vol. 276, p. 557.
15. Song, J., Lu, Y., Huang, S., et al., *Appl. Surf. Sci.,* 2013, vol. 266, p. 445.
16. Feng, L., Liu, Y., Zhang, H., et al., *Colloids Surf., A,* 2012, vol. 410, p. 66.

17. Lv, Y.Z., Wang, L.F., Ma, K.B., et al., *Adv. Mater. Res.,* 2013, vols. 641–642, p. 414.
18. Karunakaran, R.G., Lu, C.-H., Zhang, Z., and Yang, S., *Langmuir,* 2011, vol. 27, p. 4594.
19. Ming, W., Wu, D., van Benthem, R., and de With, G., *Nano Lett.,* 2005, vol. 5, p. 2298.
20. Stöber, W., Fink, A., and Bohn, E., *J. Colloid Interface Sci.,* 1968, vol. 26, p. 62.
21. Richard, E., Lakshmi, R.V., Aruna, S.T., and Basu, B.J., *Appl. Surf. Sci.,* 2013, vol. 277, p. 302.
22. Liascukiene, I., Steffenhagen, M., Asadauskas, S.J., et al., *Langmuir,* 2014, vol. 30, p. 5797.
23. Lim, M.S., Feng, K., Chen, X., et al., *Langmuir,* 2007, vol. 23, p. 2444.
24. Xue, C.-H., Jia, S.-T., Zhang, J., and Tian, L.-Q., *Thin Solid Films,* 2009, vol. 517, p. 4593.
25. Fallah, M., Rabiee, A., Ghashghaee, M., and Ershad-Langroudi, A., *Phys. Chem. Res.,* 2017, vol. 5, p. 339.
26. Xue, C.-H., Jia, S.-T., Zhang, J., and M, J.-Z., *Sci. Technol. Adv. Mater.,* 2010, vol. 11, p. 033002.
27. Ji, H., Chen, G., Yang, J., et al., *Appl. Surf. Sci.,* 2013, vol. 266, p. 105.
28. Wang, C., Zhang, M., Xu, Y., et al., *Adv. Powder Technol.,* 2014, vol. 25, p. 530.
29. Chen, Z., Tian, F., Hu, A., and Li, M., *Surf. Coat. Technol.,* 2013, vol. 231, p. 88.
30. Vo, D.Q., Kim, E.-J., and Kim, S., *J. Colloid Interface Sci.,* 2009, vol. 337, p. 75.
31. Rezayi, T. and Entezari, M.H., *J. Colloid Interface Sci.,* 2016, vol. 463, p. 37.
32. Premaratne, W.A.P.J., Priyadarshana, W.M.G.I., Gunawardena, S.H.P., and De Alwis, A.A.P., *J. Sci. Univ. Kelaniya,* 2013, vol. 8, p. 33.
33. Savva, I., Marinica, O., Papatryfonos, C.A., et al., *RSC Adv.,* 2015, vol. 5, p. 16484.
34. Scheithauer, U., *Fresenius' J. Anal. Chem.,* 1991, vol. 341, p. 445.
35. Rezayi, T. and Entezari, M.H., *New J. Chem.,* 2016, vol. 40, p. 2582.
36. Amma, S.-I., Luo, J., Pantano, C.G., and Kim, S.H., *J. Non-Cryst. Solids,* 2015, vol. 428, p. 189.
37. Charpentier, P.A., Burgess, K., Wang, L., et al., *Nanotecnology,* 2012, vol. 23, p. 425606.
38. Bywalez, R., Karacuban, H., Nienhaus, H., et al., *Nanoscale Res. Lett.,* 2012, vol. 7, p. 76.
39. Ivanova, N.A. and Philipchenko, A.B., *Appl. Surf. Sci.,* 2012, vol. 263, p. 783.